DEUTSCHES ELEKTRONEN-SYNCHROTRON DESY

DESY 83-043
June 1983

THE NONABELIAN STRUCTURE OF QCD IN QUARKONIUM DECAYS

by

K. H. Streng

Sektion Physik der Universität München

ISSN 0418-9833

NOTKESTRASSE 85 · 2 HAMBURG 52

To be sure that your preprints are promptly included in the
HIGH ENERGY PHYSICS INDEX ,
send them to the following address (if possible by air mail) :

DESY
Bibliothek
Notkestrasse 85
2 Hamburg 52
Germany

DESY 83-043
June 1983

ISSN 0418-9833

The Nonabelian Structure of QCD in Quarkonium Decays

K. H. Streng
Sektion Physik der Universität München

Abstract

We investigate beam-event correlations and transverse momentum structures for 4 jet and photon plus 3 jet decays of orthoquarkonia. Predictions depend significantly on the gluon or quark origin of the hadronic jets and on the nonabelian nature of QCD.

May 1983

1. Introduction

The e^+e^- annihilation experiments performed in the last few years at PETRA and PEP have exhibited convincing evidence for QCD as the fundamental theory of strong interactions, confirming predictions based on perturbative QCD such as jet broadening and the existence of gluon jets[2]. The ideal processes to study gluon properties are hadronic decay events of very heavy quarkonium states[3]. In fact the topology of the measured Υ decay events can only be simply understood by its decay into three coloured vector states as predicted by perturbative QCD[4]. The very good agreement between the measured angular correlation of the thrust axis and the beam axis and the theoretical value[5] for Υ decay represent an unambiguous test of the spin 1 nature of gluons[6].

To establish the nonabelian character of QCD it is necessary to measure the gluon self - coupling. In a collaboration with Koller, Walsh and Zerwas [1] (Ref. 1) it was shown [F1] that clear signals of the three gluon vertex should be visible in hadronic multijet decays of a toponium resonance[F2]. We predict multijet events from QCD multiparton subprocesses applying the following hadronization procedure. If the invariant two-parton masses of all pairs of partons in the final state are above some cutoff mass m_{cut}, then each parton fragments essentially independently into one isolated jet while parton cross sections not fulfilling this invariant mass condition contribute to higher order corrections of cross sections with lower jet multiplicity. This very simple procedure accounts quite well for the two-, three- and four - jet production in the e^+e^- continuum. That it is good enough seems hardly surprising as we are only interested in calorimetric quantities which should not sensitively depend on the evolution of soft partons and the details of confinement[F3]. The problem of jet resolution and also questions concerning higher order corrections are discussed in details in Ref. 1.

The diagrams of Fig. 1 therefore represent the QCD lowest order contribution to four jet topologies in quarkonium decay if the invariant masses of all possible two parton combinations are larger than m_{cut}. We take m_{cut} to be 5 to 7 GeV which is the mean invariant mass of hadronic jets isolated in e^+e^- continuum at 30 - 35 GeV. For a mass of the proposed toponium resonance of 40 GeV and above it should be possible to isolate such four jet decays.

The first two diagrams in Fig. 1 with four final gluons (in corresponding radiative decay one of the gluons coupled directly to the heavy quark line is replaced by a photon) contribute only if the gluons carry colour charge. These diagrams are absent in an abelian theory and represent therefore the nonabelian component of QCD. We calculated helicity amplitudes assuming static approximation for the bound state wavefunction and using standard transverse polarization vectors for the gluons. It is then possible to discuss the relative size of the contribution of the three diagrams by comparing their singularity structure (this is possible for S-wave $(Q\bar{Q})$, for details see Ref. 7). The diagram with all gluons attached to the heavy fermion line is finite for S-wave $(Q\bar{Q})$. Inspecting the well known Altarelli-Parisi formulae[8] for the splitting of a gluon into two gluons:

$$D_{G\to GG}(z,\chi) = \frac{6}{2\pi}\left\{\frac{(1-z+z^2)^2}{z(1-z)} + z(1-z)\cos 2\chi\right\} \qquad (1.1)$$

and the splitting of a gluon into a quark-antiquark pair

$$D_{G\to q\bar{q}}(z,\chi) = \frac{N_F}{2\pi}\left\{\frac{1}{2}\left[z^2+(1-z)^2\right] - z(1-z)\cos 2\chi\right\} \qquad (1.2)$$

N_F = number of quark flavours

z = momentum fraction of the outgoing parton

χ = angle of GG (or $q\bar{q}$) plane with the linear polarization of the splitting gluon

one recognizes that the four gluon final state possesses a collinear singularity (vanishing virtual gluon mass) as well as an infrared (z^{-1} bremsstrahlung singularity while in an abelian theory with only the G G q $\bar{q}$ final state of Fig. 1.c contributing there is only a collinear singularity. The main features of the hadronic four jet decay should therefore be determined by the 3-gluon vertex[F4]. This expectation is confirmed by the exact calculation. In the following all masses are given in units of the heavy quark mass.

Taking

$$m_{cut} = \frac{2}{9} \qquad (1.3)$$

(i.e. in the case of a 45 GeV toponium resonance we demand all invariant two jet masses to be larger than 5 GeV) the total decay width comes out to be about four times as large as for an abelian theory (with only the G G q $\bar{q}$ final state present and the number of light flavours equal to five), but the diagram of Fig. 1a influences this result only by a percent. In Ref. 1 we then investigated what distributions still reflect the z^{-1} bremsstrahlung singularity of $G \to G\,G$ splitting after imposing this invariant mass cut. Besides much steeper fall offs, for instance of thrust and acoplanarity distributions than one would expect from the G G q $\bar{q}$ final state, there are also clear qualitative signals. For example the energy difference between the two jets with minimal invariant mass:

$$\Delta X = \frac{|x_i - x_j|}{x_i + x_j} \qquad (k_i+k_j)^2 = m^2_{min} \qquad (1.4)$$

m_{min} : minimum of invariant masses of all two jet combinations in the event

leads to a rising distribution peaking at large Δx for QCD while it is rather flat for an abelian strong interaction theory (Fig. 3). Identifying this bremsstrahlung singularity in four jet decays and radiative photon + three jet decays experimentally will be clear evidence of the three gluon vertex (since one knows that the lowest order three jet decay originates from three vector particles).

The purpose of this work is to complete these investigations by looking for other differences between the G G G G (γ G G G) and G G q $\bar{q}$ (γ G q $\bar{q}$) final states which indicate the presence of the gluon's self - coupling. We analyze beam - event correlations and look for consequences of the different signs of the $\cos 2\chi$ terms in (1.1) and (1.2)[10].

In section 2 the reference frames chosen for the different types of decay events are specified and the six decay structure functions involved are defined. All technicalities already included in Ref. 1 are omitted. The presence of the bremsstrahlung singularity in the separate angular components of the decay width is shown in section 3. The polar angle θ between the thrust axis in (2.1)(respectively the photon momentum in (2.2)) and the beam axis should be easy to measure experimentally, how the nonabelian structure of QCD influences the predictions for these polar correlations are discussed in section 4. In section 5 we study azimuthal angular correlations between event planes which have been discussed also in four jet production in the e^+e^- continuum [9].

2. Conventions

We study beam-event correlations in heavy quarkonium decays:

$$e^+e^- \longrightarrow (Q\bar{Q})_{1^{--}} \longrightarrow \begin{cases} G(k_1) + G(k_2) + G(k_3) + G(k_4) \\ G(k_1) + G(k_2) + q(k_3) + \bar{q}(k_4) \end{cases} \qquad (2.1)$$

$$e^+e^- \longrightarrow (Q\bar{Q})_{1^{--}} \longrightarrow \begin{cases} \gamma(k_1) + G(k_2) + G(k_3) + G(k_4) \\ \gamma(k_1) + G(k_2) + q(k_3) + \bar{q}(k_4) \end{cases} \qquad (2.2)$$

The four jet decay (2.1) divides into two kinds of events with respect to the direction of the thrust axis: in Class A events the thrust axis coincides with the moments of the most energetic jet while Class B events contain two jets on each side of a plane perpendicular to the thrust axis. Our reference frames are defined in Fig. 2.In both cases the thrust axis points into the z direction and is chosen as quantization axis of the quarkonium spin. The (x,z)-plane in Class A is set by the two most energetic jets and in Class B by the fat-jet bundle that is by those two jets which point into the same hemisphere of the thrust axis and have the largest invariant mass.

In radiative decays (2.2) we put the z-axis into the direction of the photon momentum and the most energetic jet in the restframe of the hadronic recoil system defines the (x,z)-plane. In the following θ is the angle between the thrust axis and the beam and χ is the corresponding azimuthal angle of the (x,z) plane. A subscript R denotes the recoil rest frame.

The decomposition of the four jet decay width into its angular parts involves 6 decay structure functions:

$$2\pi \frac{d^2}{d\cos\theta\, d\chi}\left(\frac{1}{\Gamma_{LO}} \frac{d\Gamma}{dx_1\, dx_2^R\, dx_3^R\, d\cos\theta^R\, d\phi^R}\right) =$$

$$\frac{3}{8}\Big[(1+\cos^2\theta)\Gamma_U + 2\sin^2\theta\,\Gamma_L + 2\sin^2\theta\,(\cos 2\chi\,\Gamma_T - \sin 2\chi\,\Gamma_{TI}) - 2\sqrt{2}\,\sin 2\theta\,(\cos\chi\,\Gamma_I - \sin\chi\,\Gamma_{II})\Big] \qquad (2.3)$$

which are related to the helicity amplitudes

$$H^{\lambda_i}_{(s_z)}: \; 1^{--}(s_z) \longrightarrow \begin{cases} G(\lambda_1)\,G(\lambda_2)\,G(\lambda_3)\,G(\lambda_4) \\ G(\lambda_1)\,G(\lambda_2)\,q(\lambda_q)\,\bar{q}(\lambda_{\bar{q}}) \end{cases} \qquad (2.4)$$

by

$$\Gamma_U = C\sum_{\lambda_i}\left(H_+^{\lambda_i} H_+^{\lambda_i *} + H_-^{\lambda_i} H_-^{\lambda_i *}\right) \qquad (2.5)$$

$$\Gamma_L = C\sum_{\lambda_i} H_0^{\lambda_i} H_0^{\lambda_i *}$$

$$\Gamma_T = \frac{C}{2}\sum_{\lambda_i}\left(H_+^{\lambda_i} H_-^{\lambda_i *} + H_-^{\lambda_i} H_+^{\lambda_i *}\right)$$

$$\Gamma_I = \frac{C}{4}\sum_{\lambda_i}\left(H_+^{\lambda_i} H_0^{\lambda_i *} + H_0^{\lambda_i} H_+^{\lambda_i *} - H_-^{\lambda_i} H_0^{\lambda_i *} - H_0^{\lambda_i} H_-^{\lambda_i *}\right)$$

$$\Gamma_{TI} = -i\frac{C}{2}\sum_{\lambda_i}\left(H_+^{\lambda_i} H_-^{\lambda_i *} - H_-^{\lambda_i} H_+^{\lambda_i *}\right)$$

$$\Gamma_{II} = -i\frac{C}{2}\sum_{\lambda_i}\left(H_+^{\lambda_i} H_0^{\lambda_i *} - H_0^{\lambda_i} H_+^{\lambda_i *} + H_-^{\lambda_i} H_0^{\lambda_i *} - H_0^{\lambda_i} H_-^{\lambda_i *}\right)$$

The kinematical variables in (2.3) characterizing the event are already defined in Ref. 1 and the kinematical factor is given by:

$$C = \frac{\alpha_s}{\pi} \frac{81}{40(\pi^2-9)} \frac{x_1(1-x_1)}{4\pi \cdot S}$$

$S = 4!$ for G G G G and $2!$ for G G q $\bar{q}$.

The same decomposition holds true for the radiative decay width (2.2). The two functions Γ_{TI} and Γ_{II} vanish in lowest order three gluon decay. Their magnitude as well as the one of Γ_I is rather small and since their determination is much more involved we do not consider them here any further.

3. Bremsstrahlung -singularity

The signals of the z^{-1} bremsstrahlung singularity presented in Ref 1 for the unpolarized decay width can also be found in the corresponding distributions of the separate decay structure functions. As one example we show in Fig. 4 the dependance of Γ_u, Γ_L and Γ_T on the energy difference Δx (1.4) of the two lowest energetic jets in the 3-jet recoil rest frame of the radiative decay (2.2). The different qualitative behaviour of γ G q $\bar{q}$ and γ G G G explained in the introduction is clearly visible.

4. Polar angle distributions

The polar angle correlation between the z-axis as defined in Fig. 1 and the beam axis depends on the relative size of the unpolarized transverse and the longitudinally polarized decay structure functions Γ_u and Γ_L. Integrating out the azimuthal dependance in (2.3) we get

$$\frac{d\Gamma}{d\cos\theta} \simeq 1 + \alpha \cos^2\theta \qquad (4.1)$$

with

$$\alpha = \frac{\Gamma_u - 2\Gamma_L}{\Gamma_u + 2\Gamma_L} \qquad (4.2)$$

The experimental analysis of the dependence of α on certain kinematical quantities should not be much more involved than the determination of corresponding distributions of the unpolarized decay width. The effect of the nonperturbative p_T-smearing of the jets on α seems even less severe, at least when one considers average values of α[5]. In lowest order quarkonium decay into three gluons the values for α depend crucially on the gluon spin and we consider the fact that the measured average $\langle\alpha\rangle$ in Υ decay lies close to the predicted value $\langle\alpha\rangle \sim 39$ as a nice and unambiguous test of the vector nature of the gluons. Therefore it is interesting to study the behaviour of α in higher order contributions. One even can expect that the predictions from G G G G (γ G G G) and G G q $\bar{q}$ (γ G q $\bar{q}$) differ considerably in certain kinematical regions.

4.1 Polar angle correlation in $(Q\bar{Q}) \to 4$ jets

The values of α are restricted by helicity arguments for very small m_{min} as well as for maximal m_{min}. Let us neglect for the moment the invariant mass cut and consider extreme events with all four partons approximately collinear. The third components of the spins of an even (odd) number of transversely polarized parallel gluons can only add up to an even (odd) number and one would therefore expect the four gluon decay in this collinear limit only to occur for a longitudinally polarized quarkonium. However this is only true for the finite contribution resulting from the diagram of Fig. 1a. In the collinear limit the final state of the diagrams of Fig. 1b including a three - gluon vertex consists effectively only of three gluons. The reason for this is that the p_T-factor arizing from the above helicity argument for transversely polarized splitting gluon is cancelled by the p_T^2-factor of the gluon propagator while the longitudinal component of the virtual gluon vanishes identically in its onshell limit. These are just the well known assumptions of Weizsäcker - Williams approximations[8] and that they are fulfilled can be checked easily by inspecting the relevant formulae given in the appendix of Ref. 1. We conclude that the values of α should approach the lowest order three gluon result for very small m_{min} in the case of G G G G as well as G G q $\bar{q}$ final state. At maximal m_{min} α must vanish for all contributions. These events correspond to the symmetrical pyramid configuration and there can not be any angular correlation between thrust axis (three possible different choices) and the beam axis since we

do not discriminate between the four jets(in G G G G all final partons are identical and in G G q $\bar{q}$ we do not distinguish between a quark jet and a gluon jet).

The variation of α with m_{min} (integrated over all other kinematical variables) is shown in Fig. 5. The values are larger for G G q $\bar{q}$ than for the total QCD prediction,especially in the range $\frac{2}{9} \leq m_{min} \leq .65$. Average values of α defined by

$$\langle \alpha \rangle_{m_{cut}} = \frac{\int_{m_{cut}}^{\sqrt{\frac{2}{3}}} dm_{min} \left(\Gamma_u(m_{min}) - 2 \cdot \Gamma_L(m_{min}) \right)}{\int_{m_{cut}}^{\sqrt{\frac{2}{3}}} dm_{min} \left(\Gamma_u(m_{min}) + 2 \cdot \Gamma_L(m_{min}) \right)} \qquad (4.3)$$

are given in Table 1. In most of the α distributions we looked into there was no significant difference between the G G q $\bar{q}$ and G G G G prediction and we show only one example in Fig. 6: the variation of α with the energy of the thin-jet bundle in Class B events. The predictions of the G G G G and the G G q $\bar{q}$ final states differ more strongly when an upper cut in m_{min} is imposed.

4.2 Polar correlation in $(Q\bar{Q}) \to \gamma$ + 3jets

Radiative decays are of particular interest. They show very clean signatures and possess the important advantage that the impact from the background of

- weak t-quark decay (which becomes increasingly important for large m_t) and
- a large continuum contribution under the (t $\bar{t}$) peak is less severe. In Born approximation this is about 20 % of the gluonic decay and is large enough for a detailed analysis. In order to localize the photon in the short distance domain we use the same cuts (1.3) as applied to four jet events including the photon.

The polar angle is most suitably defined as the angle between the beam and the photon momentum.

The helicity constraints applied above to the G G G G production at very small m_{min} remain valid if one gluon is replaced by a photon. Consequently at vanishing m_{min} the values of α should approach the lowest order γ G G prediction for γ G G G as well as γ G q $\bar{q}$ - the γ G G G final state does only behave in this way if the underlying theory has the singularity structure of the three gluon vertex.

However for the symmetrical pyramid event α need no longer vanish as in four jet decay since we distinguish between the photon and a hadronic jet. In fact in an abelian theory (the G G q $\bar{q}$ contribution) Γ_u and Γ_L are identical for this event which means that α is negative: $\alpha = -\frac{1}{3}$. On the other hand for the γ G G G contribution the average values of α slightly increase with m_{cut}. The average value of α as a function of m_{min} - the minimal invariant mass of two partons or the photon and one parton in the event - is shown in Fig. 7. In an abelian theory one expects a very strong decrease of $\langle\alpha\rangle$ with m_{cut},contrary to QCD. This can be seen in Fig. 7 where we show the dependance of $\langle\alpha\rangle$ on the photon momentum for three different m_{cut} (m_{cut} = 0.1 is chosen for illustrative reasons). Note also the different behaviour of the curves in Fig. 8.c and 8.d at large x_γ which has its origin in the mentioned helicity constraints for collinear events. In table 2 we quote values of $\langle\alpha\rangle$ for different m_{cut}. It is interesting to note that from hundred events respecting $m_{cut}^2 = (\frac{2}{9})^2$ there should be about 17 (3) with $m_{min}^2 \geq \frac{1}{6}$ (0.3).

5. Azimuthal correlations inside the event

It has been argued [10] that specific transverse momentum asymmetries in quarkonium decay should occur due to the cos2χ term in the Altarelli-Parisi formulas (1.1) and (1.2). This term correlates the production plane of the emerging G G (or q$\bar{q}$) and the linear polarization of the splitting gluon. Since the virtual gluon in

$$(Q\,\bar{Q}) \to G\,G \text{ (or } \gamma G) + G^* \hookrightarrow G'\,G' \text{ and } q\,\bar{q} \qquad (5.1)$$

in fact is partly polarized perpendicular to the G G G^* (or γ G G^*) plane one expects from the sign of the cos2χ term in (1.1) and (1.2) that the G'G' plane tends to be perpendicular to the G G (γG) plane whereas q $\bar{q}$ tends to lie in the same plane as G G (γG). In an exact calculation of the four jet (photon + three jets) decay these statements will be modified and depend on the invariant mass condition which e.g. eventually will cut off more planar than spherical events.

The quantity of interest in four jet events (2.2) of Class B is the angle ϕ between the normals to the thin-jet plane and the fat-jet plane. Corresponding azimuthal distributions are proposed as a QCD test via four jet production in e^+e^- continuum [9].

For Γ_U, Γ_L and the unpolarized decay width Γ_4 one finds: if m_{cut} is very small the distributions are decreasing for increasing ϕ for G G q $\bar{q}$ but flat for G G G G. (They are rising for G G G G (G G q $\bar{q}$) if m_{cut} is larger than .1(0.3).)

In the case of Γ_T there are kinematical regions in which the linear polarization of the virtual gluon is very large (for details see Ref. 11). The resulting ϕ dependance is rapidly falling for G G q $\bar{q}$ and flat for G G G G even at very large m_{cut}. The predictions for $m_{cut} = \frac{2}{9}$ are shown in Fig. 9.

A corresponding quantity in the radiative decay (2.2) is the angle χ between the normal to the plane given by the photon and the fastest jet in the hadronic recoil restframe and the normal to the plane of the two other jets. The qualitative behaviour of the resulting χ distributions of Γ_U, Γ_L and the unpolarized decay width $\Gamma_{3\gamma}$ is similar to that discussed above. There is however already a rise in the total prediction for $\Gamma_{3\gamma}$ at $m_{cut} = \frac{2}{9}$. In the case of Γ_T once again for γ G q $\bar{q}$ the distribution is strongly decreasing even at high m_{cut} but for γ G G G it is flat at small m_{cut} and strongly rising at large m_{cut}. Predictions for $m_{cut} = \frac{2}{9}$ are shown in Fig. 10.

Conclusion

Multijet hadronic decays of a very heavy quarkonium state should allow very clean tests of all the ingredients of QCD. Beam-event correlations of the three-jet (photon + 2-jet) final state and the four-jet (photon + 3-jet) final state will show that in all cases the dominant subprocesses involve only vector states. The signals of the infrared bremsstrahlung singularity discussed here and in reference [1] will verify the nonabelian nature of QCD.

Acknowledgement

The author thanks T. Walsh for the hospitality of the DESY theory group and for his comments. He thanks P. Zerwas for useful discussions.

Footnotes

F1: The part of the numerical program which calculated the G G G G predictions in four jet decay shown in Ref. 1 had a small error. The change of the shapes of the curves presented in Ref. 1 is negligibly small. We include here with Fig. 3 the corrected Δx distributions replacing Fig. 7 of Ref. 1 (Δx defined by (1.4). The normalization of four-jet decays compared to lowest order G G G decay width increases from $13\,\frac{\alpha_s}{\pi}$ to $17\,\frac{\alpha_s}{\pi}$ for $m_{cut} = \frac{2}{9}$.

We also want to mention two evident misprints in the formulae given in the appendix of Ref. 1: On page 294 in the definition of R (123;4) the second ϵ_2 of the first term has to be replaced by ϵ_3 and on page 295 the factor x_3 in c_{oo}^1 has to be replaced by x. Interested readers may request the four FORTRAN-Generators we have written for the four decay modes (2.1) and (2.2).

F2: Heavy quarkonium decays into four jets were recently also studied by Muta and Niuya [12].

F3: However precise measurements of e.g. α_s will depend on the details of confinement [13]. Note that by contrast gluon spin tests are unaffected, as we would expect.

F4: Koller, Walsh and Zerwas [14] showed that for this reason the evolution of single particle spectra (or their moments) from one onium state to the next also measures the three-gluon vertex.

REFERENCES

1. K. Koller, K. H. Streng, T.F. Walsh and P.M. Zerwas, Nucl. Phys. B 206 (1982) 273.

2. R. Brandelik et al., Phys. Lett. 86B (1979) 243; D.P. Barber et al., Phys. Rev. Lett. 43 (1979) 830; C. Berger et al., Phys. Lett. 86B (1979) 418; W. Bartel et al., Phys. Lett. 91B (1980) 142.

3. K. Koller and T.F. Walsh, Phys. Lett. 72 B (1977) 227; S. Brodsky et al., Phys. Lett. 73 B (1978) 203; H. Fritzsch and K. Streng, Phys. Lett. 74 B (1978) 90.

4. K. Koller and H. Krasemann, Phys. Lett. 88 B (1979) 119. T.F. Walsh and P.M. Zerwas, Phys. Lett. 93 B (1980) 53.

5. K. Koller, H. Krasemann and T.F. Walsh, Z. Physik C1 (1979) 71.

6. Ch. Berger et. al., Z. Physik C8 (1981) 101 B. Niczyporuk et al., Z. Physik C9 (1981) 1 M. Gilchriese, Proceedings of the 2nd International Conference on Physics in Collisions, Stockholm, June 1982

7. K. Koller, K.H. Streng, T.F. Walsh and P.M. Zerwas, Nucl. Phys. B 193 (1981) 61.

8. G. Altarelli und G. Parisi, Nucl. Phys. B 126 (1977) 298

9. J.G. Körner, G. Schierholz and J. Willrodt, Nucl. Phys. B 185 (1981) 365.

10. S. Brodsky, T. De Grand and R. Schwitters, Phys. Lett. 79B (1978) 225.

11. J.G. Körner and D. McKay, Z. Phys. C9 (1981) 67.

12. T. Muta and T. Niuya, Prog. Theor. Phys. 68 (1982) 1735.

13. H.J. Behrend et al., DESY 82/61 (1982).

14. K. Koller, T.F. Walsh and P.M. Zerwas, Phys. Lett. 82B (1979) 263.

Figure Captions:

Fig. 1 Orthoquarkonium decay into G G G G and G G q $\bar{q}$. Permutations of gluon lines are not shown.

Fig. 2 Coordinate systems chosen to define angular correlations for
(a) $(Q\bar{Q}) \to$ 4-jets : Class A
(b) $(Q\bar{Q}) \to$ 4-jets : Class B
(c) $(Q\bar{Q}) \to \gamma$ + 3 jets.

Fig. 3 Δx -distribution (Δx as defined by (1.4)) of the unpolarized 4-jet decay-width. Minimum invariant mass m_{min} between $\frac{2}{9}$ and $\frac{3}{9}$. Here and in the following plots the curves are smooth interpolations through the Monte Carlo data points.

Fig. 4 Δx -distribution for the angular parts Γ_U, Γ_L and Γ_T of decay $(Q\bar{Q}) \to \gamma$ + 3-jets normalized to radiative Born term decay width in units of $\frac{\alpha_s}{\pi}$. Minimum invariant mass m_{min} between $\frac{2}{9}$ and $\frac{3}{9}$.

Fig. 5 Average values of the coefficient α of the polar angle for 4-jet decay as function of m_{min}.

Fig. 6 $\langle\alpha\rangle$ for Class B events as function of the energy of the thin-jet bundle in its own c.m.s. Predictions are shown for m_{min} between $\frac{2}{9}$ and $\frac{3}{9}$ and for m_{min} larger $\frac{2}{9}$.

Fig. 7 Average values of the photon polar angle coefficient α for $(Q\bar{Q}) \to \gamma$ + 3-jets as function of m_{min}.

Fig. 8 $\langle\alpha\rangle$ for $(Q\bar{Q}) \to \gamma$ + 3-jets as function of the photon momentum for three different invariant mass cuts: $m_{cut} = 0.1$, $m_{cut} = \frac{2}{9}$ and $m_{cut} = \sqrt{0.3}$.
(a) total QCD prediction
(b) only G G q $\bar{q}$ final state
(c) only G G G G final state
(d) prediction from the diagram of Fig. 1a only.

		ALL EVENTS			CLASS A			CLASS B		
		$\frac{2}{9} \le m_{min}$	$\frac{2}{9} \le m_{min} \le \frac{3}{9}$	$\frac{3}{9} \le m_{min}$	$\frac{2}{9} \le m_{min}$	$\frac{2}{9} \le m_{min} \le \frac{3}{9}$	$\frac{3}{9} \le m_{min}$	$\frac{2}{9} \le m_{min}$	$\frac{2}{9} \le m_{min} \le \frac{3}{9}$	$\frac{3}{9} \le m_{min}$
$\langle\alpha\rangle$	QCD	.35	.36	.32	.31	.32	.28	.36	.38	.33
	$GGq\bar{q}$	.40	.41	.39	.33	.35	.27	.43	.45	.42
	GGGG	.33	.35	.30	.30	.31	.28	.34	.37	.30
$\Gamma_{4j}/\Gamma_{L.O.}$		$17\frac{\alpha_s}{\pi}$	$11\frac{\alpha_s}{\pi}$	$6\frac{\alpha_s}{\pi}$	$5\frac{\alpha_s}{\pi}$	$4\frac{\alpha_s}{\pi}$	$1\frac{\alpha_s}{\pi}$	$12\frac{\alpha_s}{\pi}$	$7\frac{\alpha_s}{\pi}$	$5\frac{\alpha_s}{\pi}$
$\Gamma_{GGq\bar{q}}/\Gamma_{4j}$		.24	.21	.28	.23	.22	.27	.24	.20	.28

Table 1: Average values of α in four-jet decays (2.1) for three different ranges of m_{min}. Predictions are shown seperately for decays into G G q $\bar{q}$ and G G G G final states and the total QCD result for five light flavours. The last two columns present the normalization compared to the decay width in lowest order and the fraction of G G q $\bar{q}$ events.

Fig. 9 Azimuthal angular distribution ϕ between the thin-jet plane and the fat-jet plane of the transverse - interference decay structure function Γ_T of 4-jet Class B events, m_{min} larger $\frac{2}{9}$.

Fig. 10 For $(Q\bar{Q}) \to \gamma$ + 3-jets: azimuthal angular distribution χ between the plane of γ and fastest jet in the hadronic restframe and the plane of the two other jets, m_{min} larger $\frac{2}{9}$.
(a) unpolarized decay width $\Gamma_{3\gamma}$
(b) transverse - interference decay structure function Γ_T.

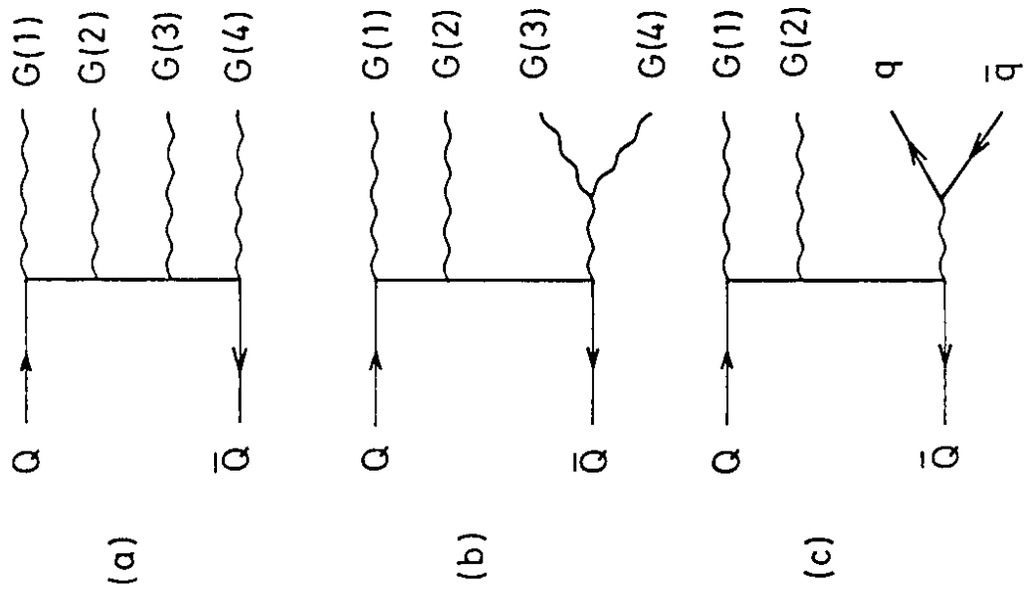

Fig.1

m_{cut}		0.1	2/9	3/9	$\frac{1}{\sqrt{6}}$	$\sqrt{.3}$	0.63
$\langle\alpha\rangle$	QCD	0.35	0.34	0.32	0.31	0.30	0.29
	$\gamma G_{q\bar{q}}$	0.32	0.26	0.20	0.15	0.04	-0.05
	γGGG	0.35	0.36	0.36	0.37	0.39	0.41
$\Gamma_{\gamma 3G}/\Gamma_{\gamma 2G}$		$44\,\frac{\alpha_s}{\pi}$	$14.4\,\frac{\alpha_s}{\pi}$	$5{,}3\,\frac{\alpha_s}{\pi}$	$2{,}5\,\frac{\alpha_s}{\pi}$	$.4\,\frac{\alpha_s}{\pi}$	$.07\,\frac{\alpha_s}{\pi}$
$\Gamma_{\gamma G q\bar{q}}/\Gamma_{\gamma 3G}$		0.14	0.19	0.22	.24	.24	.24

Table 2: Average values of α in radiative decays (2.2) for different invariant mass cuts. Predictions are shown seperately for decays into γ G q $\bar{q}$ and γ G G G final states and the total QCD result for five light flavours. The last two columns present the normalization compared to the decay width in lowest order γ G G and the fraction of γ G q $\bar{q}$ events.

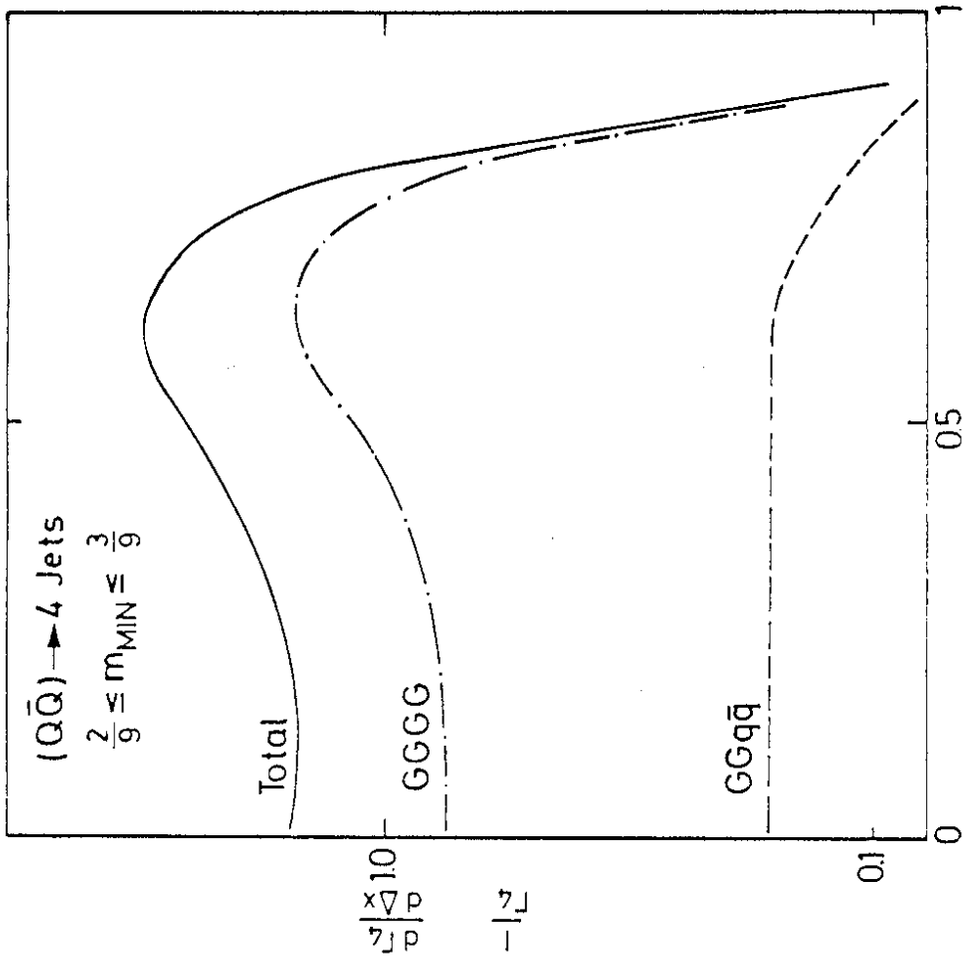
$(Q\bar{Q}) \rightarrow 4$ Jets
$\frac{2}{9} \leq m_{MIN} \leq \frac{3}{9}$
Total
GGGG
GGqq̄
$\frac{1}{\Gamma_4}$
$\frac{d\Gamma_4}{d\Delta x}$
10
01
0
05
1
Δx

Fig. 3

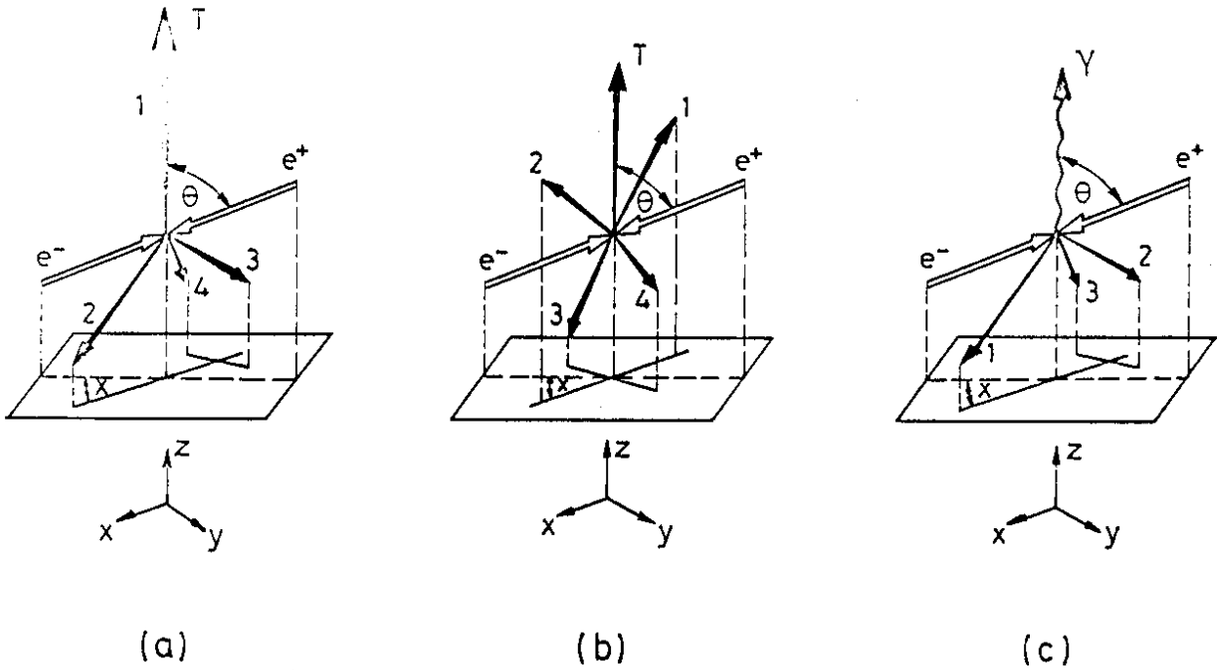
T
1
e+
e-
Θ
2
3
4
χ
z
x
y
(a)
T
1
2
e+
e-
Θ
3
4
χ
z
x
y
(b)
γ
e+
e-
Θ
2
3
1
χ
z
x
y
(c)

FIG. 2

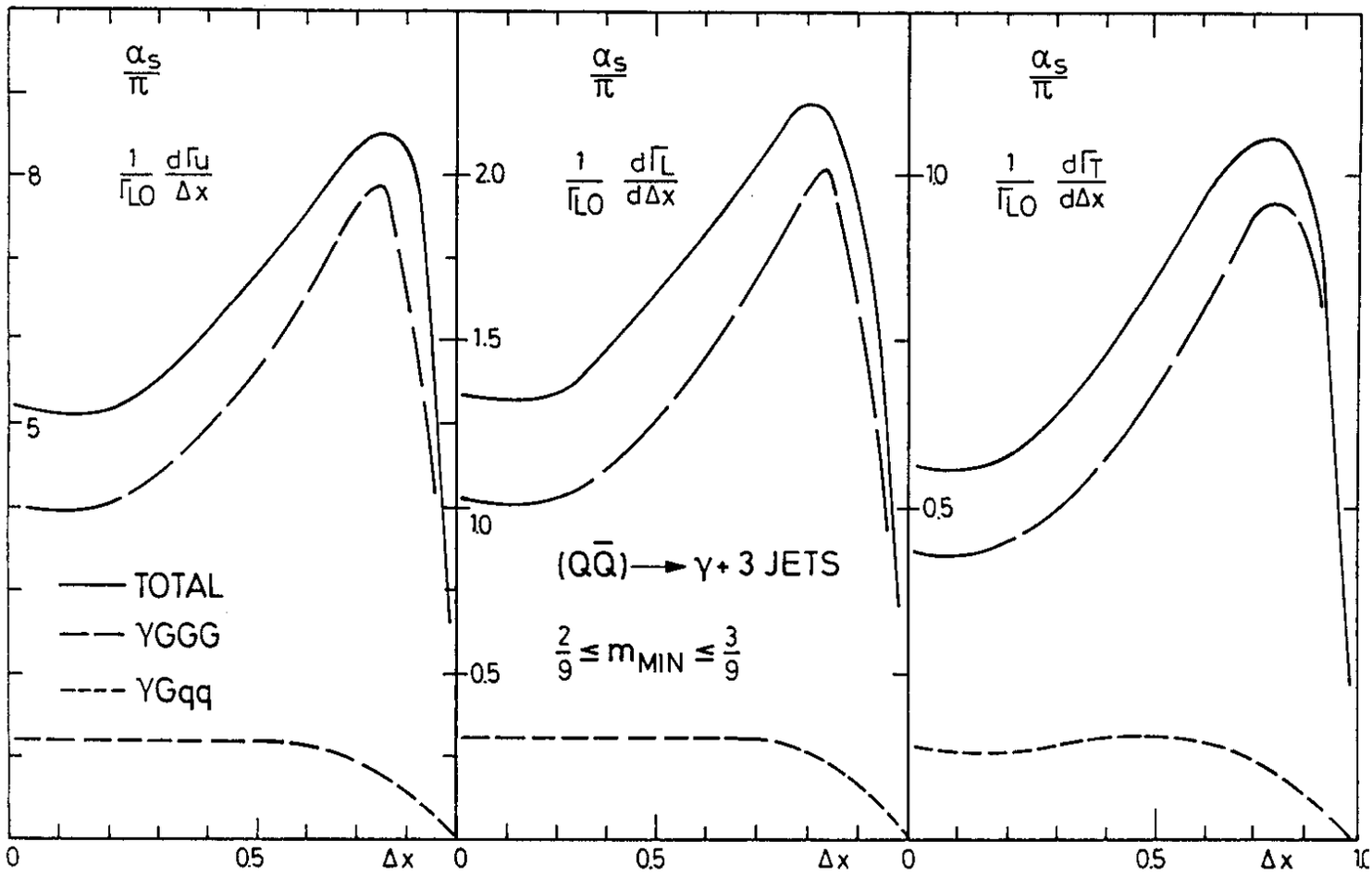

FIG. 4

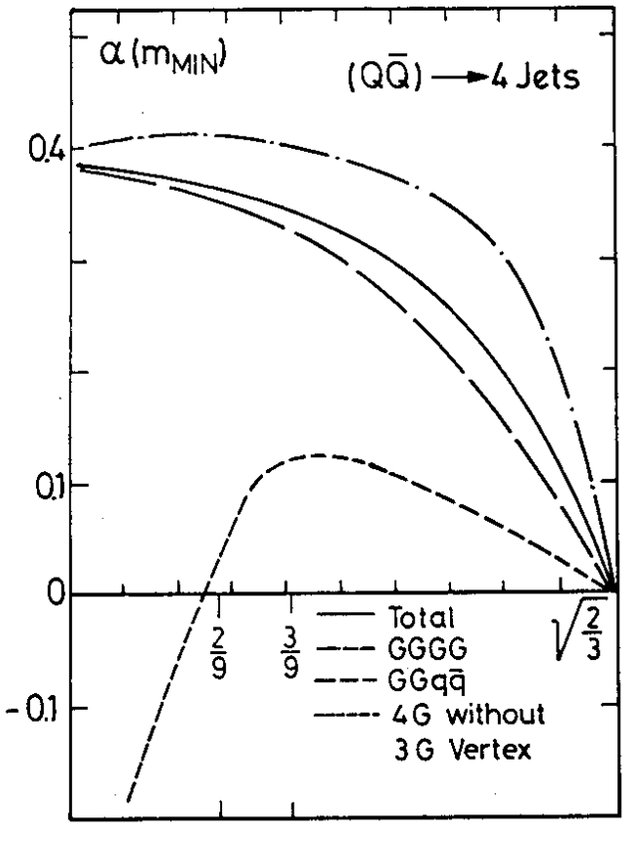

Fig. 5

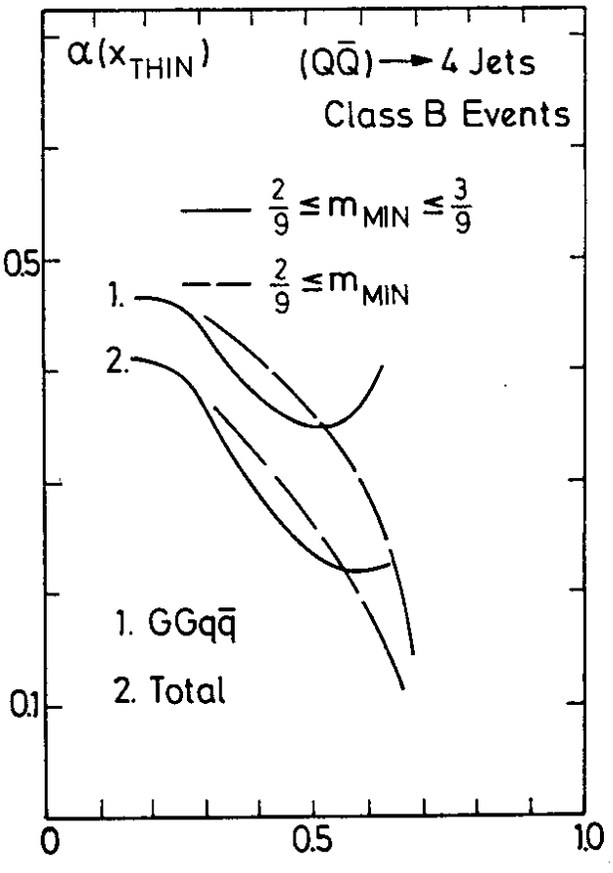

Fig. 6

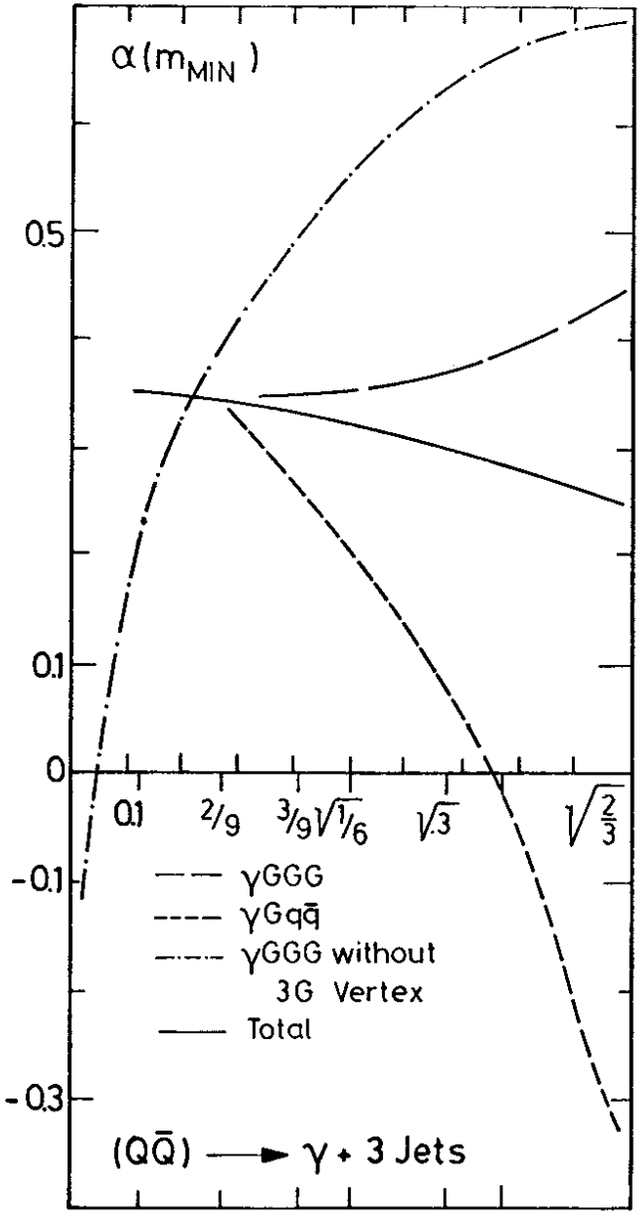
α(m_MIN)
0.5
0.1
0
-0.1
-0.3
0.1
2/9
3/9√1/6
√3
√2/3
γGGG
γGqq̄
γGGG without 3G Vertex
Total
(QQ̄) → γ + 3 Jets

Fig. 7

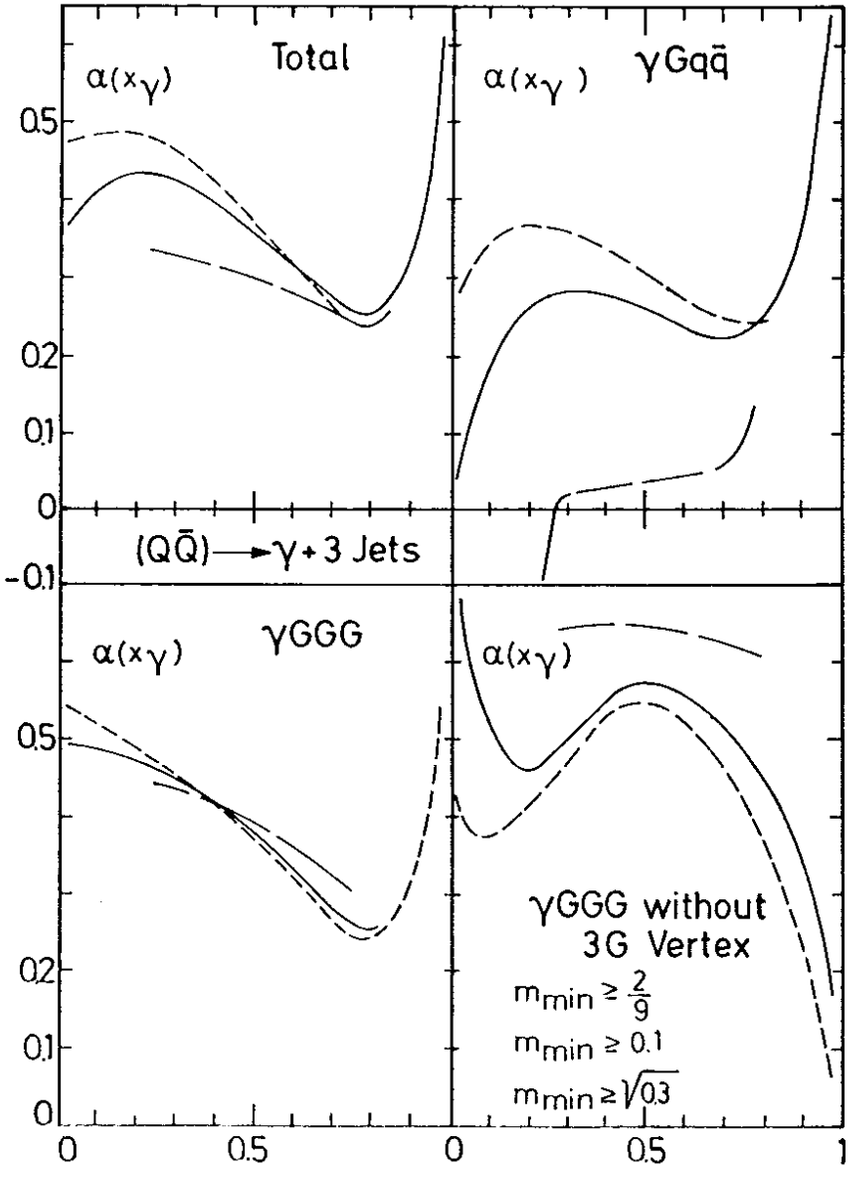
α(x_γ)
Total
α(x_γ)
γGqq̄
0.5
0.2
0.1
0
-0.1
(QQ̄) → γ + 3 Jets
α(x_γ)
γGGG
α(x_γ)
γGGG without 3G Vertex
m_min ≥ 2/9
m_min ≥ 0.1
m_min ≥ √0.3
0
0.5
0
0.5
1

Fig. 8

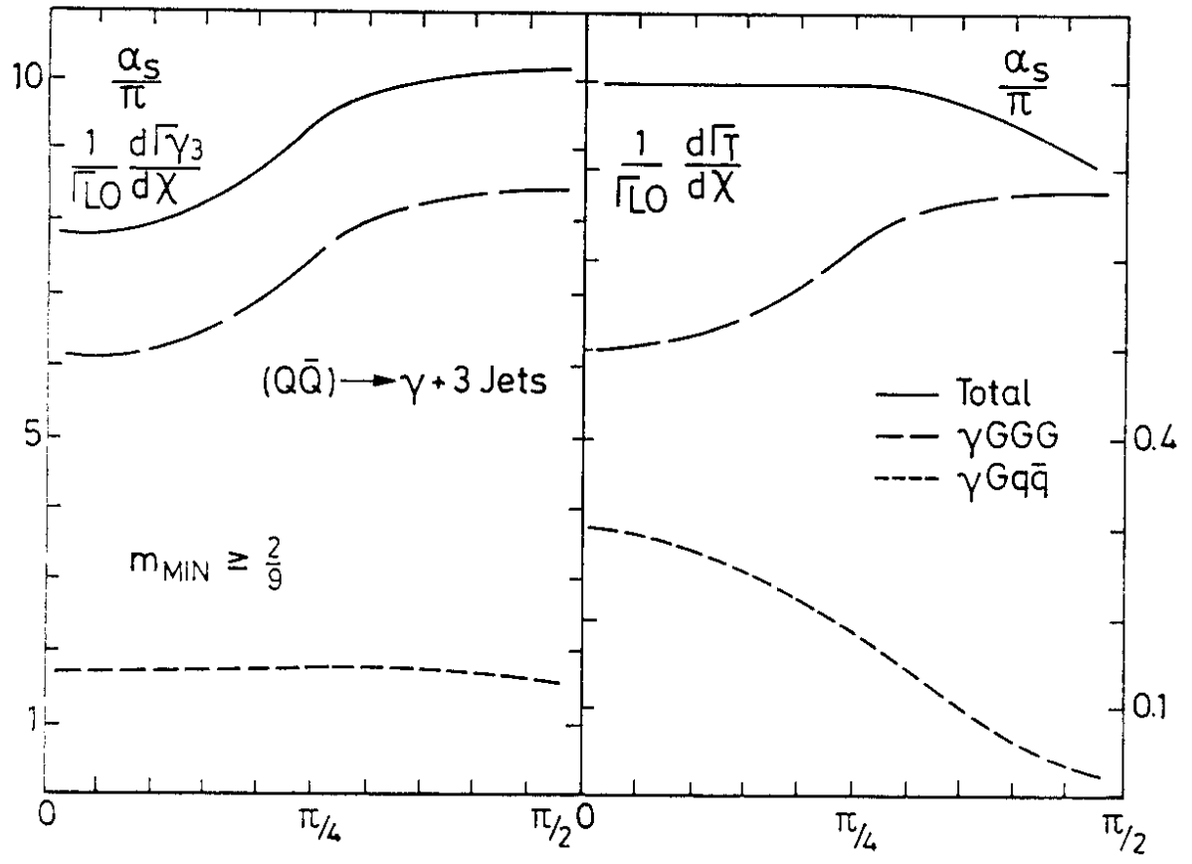
10
5
1
$\frac{\alpha_s}{\pi}$
$\frac{1}{\Gamma_{LO}}\frac{d\Gamma_{\gamma 3}}{dX}$
$(Q\bar{Q}) \longrightarrow \gamma + 3$ Jets
$m_{MIN} \geq \frac{2}{9}$
$\frac{\alpha_s}{\pi}$
$\frac{1}{\Gamma_{LO}}\frac{d\Gamma_T}{dX}$
Total
γGGG
$\gamma Gq\bar{q}$
0.4
0.1
0
$\pi/4$
$\pi/2$
0
$\pi/4$
$\pi/2$

Fig. 10

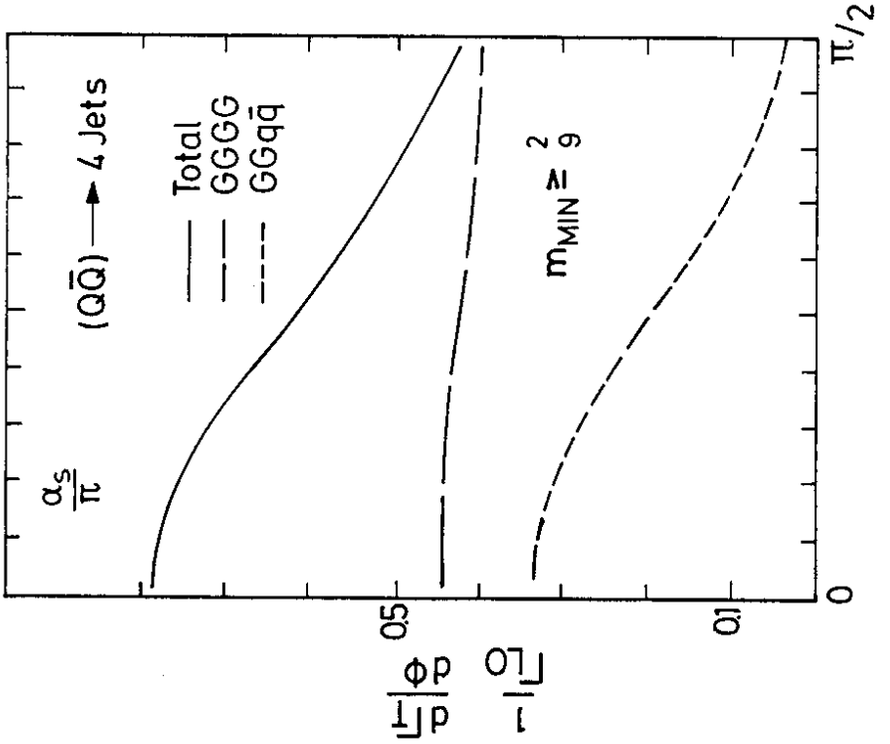
$\frac{\alpha_s}{\pi}$
$(Q\bar{Q}) \longrightarrow$ 4 Jets
Total
GGGG
$GGq\bar{q}$
$m_{MIN} \geq \frac{2}{9}$
$\frac{1}{\Gamma_{LO}}\frac{d\Gamma_T}{d\phi}$
0.5
1.0
0
$\pi/2$

Fig. 9